Available online at www.sciencedirect.com

ScienceDirect

Energy Procedia 57 (2014) 14 – 23

Energy Procedia

2013 ISES Solar World Congress

Analysis of PV modules and n-type silicon solar cells with different rear metal grid

Izete Zanesco*, Sérgio B. Garcia, Adriano Moehlecke and Moussa Ly

Solar Energy Technology Nucleus (NT-Solar), Faculty of Physics, Pontifical Catholic University of Rio Grande do Sul (PUCRS), Av. Ipiranga, 6681, Prédio 96A, Porto Alegre – RS, CEP 90619-900, Brazil

Abstract

N-type silicon solar cells are being investigated due to the potential to obtain high efficiency. In this solar cell, the front p^+ emitter is performed with boron doping and the Al or Al/Ag screen printing pastes don't reach the development of Ag pastes used to form the front contact in n^+pp^+ solar cells. Moreover, the rear area covered by metal grid on the phosphorus back surface field may be optimized to increase the silicon solar cell efficiency and reduce the cost production. The goal of this paper is to present the analysis of PV modules and silicon solar cells developed on phosphorus-doped Czochralski wafers with different metal grid on the rear face. The solar cells were processed by using spin-on dopant to obtain the boron emitter and the back surface field was formed by phosphorus diffusion. The front metal grid was formed with Al/Ag paste and the rear area covered by the Ag metal paste was varied from 9 % to 53 %. Solar cells were manufactured, characterized and sorted taking into account the short-circuit current. Eight PV modules were fabricated using a standard process. Solar cells presented low fill factor. When the Ag/Sn/Cu ribbon was soldered on the front busbars of a solar cell, the fill factor rose from 0.70 to 0.75, causing an increase of 13.2 % to 15.0 % in the efficiency. Therefore, the fill factor of the PV modules was higher than that of solar cells. The reduction of the metal grid area on the rear face of solar cells did not affect the fill factor and solar cells with low rear metal coverage presented higher short-circuit current. The infrared thermography analysis was performed under a cloudless sky day with modules in the short-circuit condition. All modules presented hot spots and this result was not related to the different metallized rear area. The temperature difference between the solar cells of each photovoltaic module varied from 9 °C to 18 °C.

Keywords: n-type silicon solar cells; PV modules; rear metal grid

* Corresponding author. Tel.: +55 51 33203682; fax: + 55 51 33203616.
E-mail address: izete@pucrs.br.

doi:10.1016/j.egypro.2014.10.003

1. Introduction

The goal of the PV industry is to reduce the cost production to achieve the grid parity. Active investigations are being performed to reduce the cost of kWp, such as, the cost reduction of raw material, the increasing of the efficiency of solar cells with low cost techniques, the use of solar grade Si substrates, the reduction of the thickness of Si wafers, the increasing of the scale production, the research on n-type silicon wafers and others.

The PV industry is dominated by silicon solar cells fabricated in Czochralski-grown (Cz-Si) p-type substrate with aluminum back surface field (Al-BSF) formed by Al paste screen-printed and fired in a belt furnace. In this kind of solar cells, there are two main problems to overcome: the Al-BSF rear passivation technology limits the efficiency mainly in thin substrates [1] and the screen-printed Al paste produces bowing of the wafer, despite of the evolution of low-bow pastes [2].

In the last 13 years, the share market of silicon solar cells was around 87 %, taking into account mono and multicrystalline silicon devices [3]. In the last years, the industrial production of n-type monocrystalline Si solar cells had increased and the market share is about 4 % [4]. The research in n-type solar cells had been attractive due to the potential to obtain high efficiency. Substrates doped with phosphorus are more stable, present high tolerance to metallic impurities, can have higher minority charge carrier lifetimes than p-type silicon, the bowing can be avoided if p^+ region is doped with boron and the rear surface can be passivated [5] e [6]. For these reasons, cost-effective technologies for n-type Si solar cells are under investigation. The main structures investigated to produce n-type Si solar cell are: front side boron emitter, aluminum rear side emitter, interdigitated back contact (IBC) and heterojunction with intrinsic thin layer (HIT).

High efficiency was achieved using n-type Si solar cells. The back-contacted and back-junction with interdigitated contact solar cell with area of 155.1 cm^2 and processed in n-type Cz wafers reached the efficiency of 24.2 % [7]. New results have been reported on solar cells with interdigitated metal fingers evaluating the large and small emitter coverage. For instance, silicon solar cells processed in n-type float-zone grown wafers with Al metal fingers evaporated by electron beam presented the efficiency of up to 23.0 %, when the SiO_2 layer and passivation were optimized [8]. A back-contact back-junction solar cell was developed with an aluminum-alloyed emitter and metallization by screen printing, resulting in the efficiency of 19.7 %. In this research, different emitter coverage on the rear side (45 %, 58 %, and 72 %) was evaluated [9].

Heterojunction solar cell with intrinsic thin layer achieved the efficiency of 23.7 % [10]. Yingli's PANDA solar cells fabricated in n-type CZ wafers achieved an average efficiency on commercial production lines exceeding 19.0 % and up to 20.0 % in pilot production [6].

N-type PERL (passivated emitter, rear locally-diffused) solar cells with a low doped boron emitter and a SiO_2 rear passivation lead to an efficiency of 23.4 % [11]. When the negatively-charged dielectric Al_2O_3 was applied to passivated the rear surface, silicon solar cells achieved the efficiency of 23.2 % [12].

The current processes for the p^+ emitter formation can result in unintentional supersaturated boron-rich layer. Ryu et al. [13] reported an increase of 1.6 % in the efficiency (absolute) if a chemical etching of boron-rich layer is performed and the 19.0 % efficiency in a large area (239 cm^2) Cz n-type Si solar cell was achieved.

A process was developed to fabricate n-type solar cells (156.25 cm^2) in multicrystalline substrates with simultaneous diffusion of phosphorus and boron to form the back surface field and emitter, that lead to the efficiency of 16.4 % [14]. A maximum efficiency of 15.0 % was obtained in solar cells processed in solar grade n-type multicrystalline silicon purified via the metallurgical route [15].

Photovoltaic (PV) modules assembled with n-type silicon solar cells had been developed. The main advantages are the absence of light induced degradation effects and the potential to obtain high efficiency.

Some industries are fabricating PV modules with this kind of solar cells. A vertically integrated module production from n-type Cz-Si crystal growth, wafer slicing, cell processing and module assembly was developed by Yingli [6]. The PANDA technology was developed to achieve the lowest manufacturing cost of Wp. The PANDA modules presented superior high temperature performance with temperature coefficients that are 6 % - 9 % lower than those for conventional p-type Si modules.

Sanyo commercializes the 240 W module with 19 % efficiency by using HIT cells in volume production [16]. This efficiency was achieved by redesigning the tabs and using anti-reflection coated glass. The efficiency of HIT solar cells reached 21.6 %.

SunPower Corporation had fabricated a high-efficiency PV module assembled with IBC solar cells. The commercial 330 W solar module achieved the efficiency of 20.4 % [7].

Bifacial solar cells can be produced by using n-type silicon wafers and front boron emitter. Modules produced with bifacial solar cells can convert the solar energy that reached on front and rear side. For example, the bifacial PANDA module produces around of 15 % more electric power than the single-sided PANDA module, if mounted on a roof with a white color [6].

Bearing in mind the active research in n-type silicon solar cells and modules, the goal of this paper is focused on the development and analysis of PV modules and n-type silicon solar cells with boron doped emitter processed in solar grade Czochralski (Cz) wafers. To analyze how screen-printed metal grid on the rear n^+ BSF may affect the cell efficiency and the performance of the PV modules, the rear area covered with Ag paste was varied from 9 % to 53 %. Concerning the PV modules, the hot spots were investigated by thermographic technique.

2. Manufacturing processes

2.1. Silicon solar cells

Solar cells were developed in 1 Ω.cm – 20 Ω.cm n-type solar grade Cz-Si wafers with thickness of 200 μm. The baseline process was: texture etching, RCA cleaning, boron spin-on deposition, boron diffusion in a quartz tube furnace and oxidation, resist deposition and oxide etching, RCA cleaning, phosphorus diffusion, borosilicate glass etching, TiO_2 anti-reflection coating deposition, screen printing metallization in both sides and edge isolation. A specific passivation was not implemented. The rear metal grid is similar to the front metal grid and it was formed by two busbars that connect the fingers ("H" pattern).

The boron dopant was spun onto one side of the wafer and the diffusion was carried out in a quartz tube furnace at 1000 °C. The n^+ layer was performed by phosphorus diffusion using $POCl_3$. The oxide used as a barrier to phosphorus diffusion was grown in the same thermal step of boron diffusion and this step was experimentally optimized.

The boron emitter (B-emitter) and phosphorus BSF (P-BSF) were experimentally and independently optimized as well as the simultaneous firing process of the front (Ag/Al) and rear (Ag) pastes. The diffusion processes formed a (39.6 ± 0.6) Ω/□ p^+ emitter and a (18.9 ± 0.4) Ω /□ n^+ layer. In Fig. 1 the boron and phosphorus profiles measured by ECV (electrochemical capacitance-voltage) technique are shown. The surface concentration of the boron doped emitter is lower than the phosphorus BSF. The junction depth for p^+ emitter was around 0.8 μm and it is deeper than the thickness of BSF region, which was approximately 0.6 μm. On the other hand, the surface concentration of boron (~ $1.5x10^{19}$ atoms/cm^3) was lower than that of phosphorus profile (~ $2.5x10^{20}$ atoms/cm^3).

All the devices were characterized under standard conditions (100 mW/cm^2, AM1.5G and 25 °C) in a solar simulator calibrated with a solar cells previously measured at CalLab - FhG-ISE (*Fraunhofer-Institut für Solare Energiesysteme*), Germany.

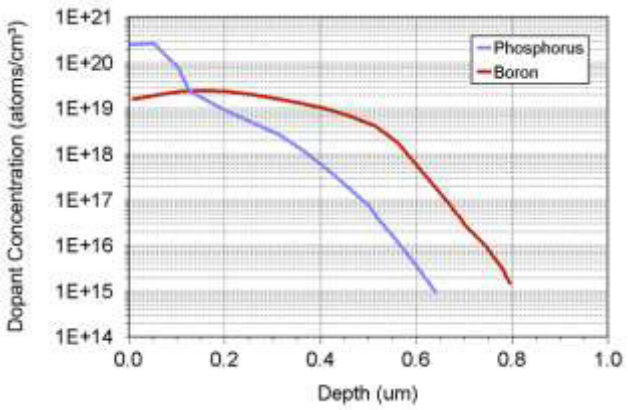

Fig. 1. Boron and phosphorus profile of p^+nn^+ (B-emitter) silicon solar cells measured by ECV technique.

2.2. PV modules

Eight PV modules were fabricated using the standard process of the PV industry based on tempered high transmittance glass (3.2 mm thick), fast cure EVA (ethylene vinyl acetate) and backsheet. Modules consist of four strings with nine cells and the area of the modules was 0.277 m^2.

PV modules were assembled by using n-type solar cells with different area covered by the rear metal grid. Some modules were fabricated using solar cells with different coverage of metal grid to evaluate hot spots in the same PV module.

The cell strings were soldered in an automatic tabber-stringer equipment. The process of soldering tabs and to connect cells to produce the strings was optimized taking into account the ribbon, the metal paste and the fluxant. To connect string to string, a specific mask was used to allow the alignment of the strings during the soldering process.

The module lamination-curing process profile, that involves several steps at different temperatures, was optimized to obtain cured EVA film with 90 % of gel content. This value is higher than the range of 65 % to 80 % accepted to produce long lifetime modules [17], [18]. Backsheet based on Tedlar® (38 μm), PET (125 μm) and primer (100 μm) was used, producing good isolation for voltages up to 1000 V. Glass sheets were washed with de-ionized water in a system based on a cascade with three recipients.

Anodized aluminum frame was manually assembled by using a pneumatic tool that pressed simultaneously the four parts of the frame, rivets and silicone (specific for PV purpose) to seal the edges. Junction box with two diodes, each protecting two strings of nine cells, was attached to the module. All modules received a label (bar code) with information about solar cells and the materials used.

3. Analysis of n-type silicon solar cells

N-type solar cells were processed with different Ag paste coverage on the rear face that was decreased from 53 % to 9 % to reduce the cost production and to assess the influence on the efficiency of the solar cells and on the performance of the PV modules. The solar cells with a rear metal coverage of 9 %, 14 % and 53 % were denominated of SC-grid-9%-38f (38 metal fingers), SC-grid-14%-76f (76 metal fingers), SC-grid-53%-400f (400 metal fingers), respectively.

Solar cells were sorted in four categories concerning J_{SC} as presented in Table 1. This classification is currently used because cells are connected in series in most PV modules. Only solar cells with FF higher than 0.70 were selected, because the fill factor was lower than that expected due to the higher resistivity

of the Ag/Al paste used to perform the front metal grid. This paste is commonly used to form the rear metallization in n^+pp^+ solar cells. However, when the Ag/Sn/Cu ribbon was soldered on the front busbars of the solar cells, the fill factor rose from 0.70 to 0.75, causing an increase of 13.2 % to 15.0 % in the efficiency, as shown in Fig. 2.

Table 1. Classification of the B-emitter solar cells used to fabricate the PV modules.

Class	J_{SC} (mA/cm^2)
A	≥ 32
B	$31 \leq J_{SC} < 32$
C	$30 \leq J_{SC} < 31$
D	$29 \leq J_{SC} < 30$

Fig. 3 presents the reflectance of the TiO_2 AR coating, experimentally optimized in order to obtain the higher J_{SC}. The reflectance was measured in a wafer with AR coating and without metal grid and processed in a belt furnace with the same parameters used to fire the screen-printed metal pastes. The minimum reflectance of 0.6 % occurs in the wavelength range of 770 nm to 810 nm. This result is related to the poor response of the solar cell due to the high recombination and the lack of an effective passivation of the p^+ emitter, as confirmed by the internal quantum efficiency, shown in Fig 4. The surface recombination velocity of the p^+ region obtained from the internal quantum efficiency simulated by PC-1D (one-dimensional solar cell device simulator) was $1x10^7$ cm/s.

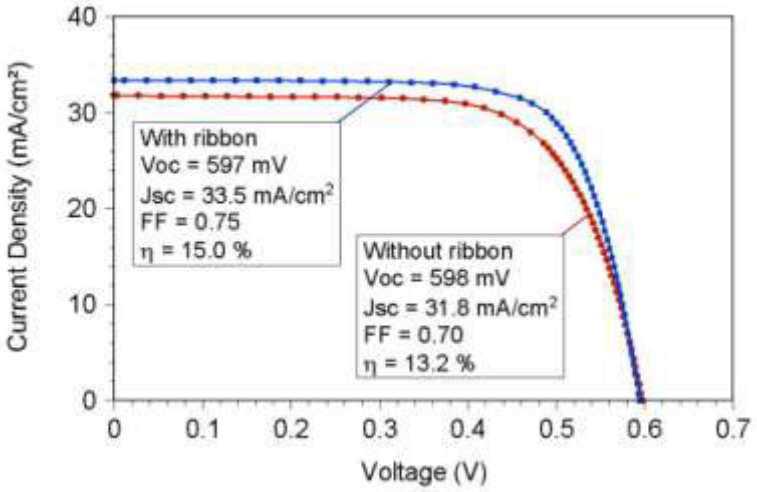

Fig. 2. Electric current density as a function of applied voltage, measured under standard conditions of n-type solar cell without and with an Ag/Sn/Cu ribbon soldered on the front busbars.

The J-V curves of three solar cells with rear metal coverage of 9 %, 14 % and 53 % produced in the same batch are plotted in Fig. 5. The V_{OC} and FF are similar. The solar cell SC-grid-53%-400f presented lower J_{SC} than cells SC-grid-9%-38f and SC-grid-14%-76f, because the lower reflectance at longer wavelengths caused by the increase of the area covered by the Ag paste on the rear face [19].

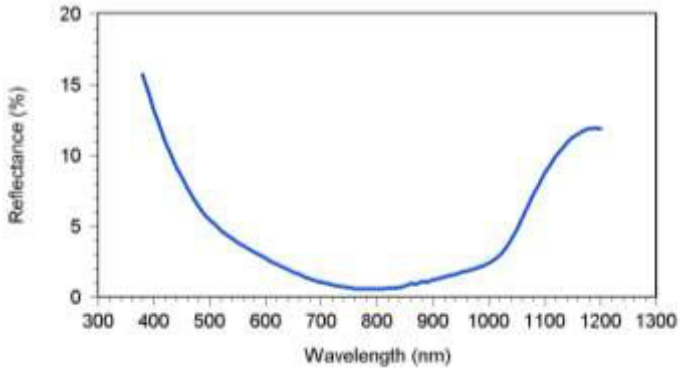

Fig. 3. Reflectance of the TiO_2 AR coating experimentally optimized and measured after the firing at temperature of 840 °C without the deposition of the metal grid.

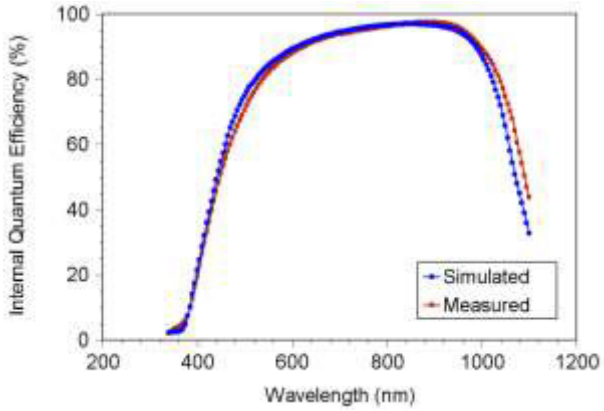

Fig. 4. Internal quantum efficiency measured and simulated by using the PC-1D computer program.

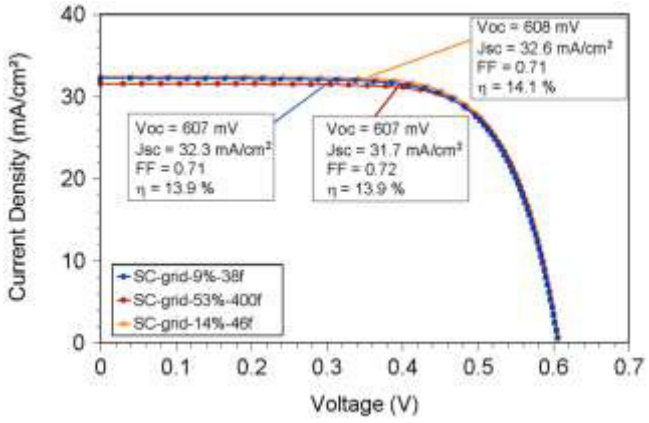

Fig. 5. Electric current density as a function of applied voltage measured under standard conditions of B-emitter solar cell with different rear metal coverage.

4. Analysis of PV modules

4.1. Electrical characterization

All modules were characterized under standard conditions (1000 W/m^2, AM1.5G, 25 ºC) by using a flash solar simulator class AAA. Solar simulator was calibrated with a PV module previously calibrated in the European Solar Test Installation (ESTI), Joint Research Center - European Community, Italy. Table 2 presents the average values of the open circuit voltage, short-circuit current, fill factor and maximum power (P_{MPP}) of the eight fabricated modules as well as the solar cells used (class and metal coverage of rear face). Two PV modules (4 and 8) were assembled with different classes of solar cell to investigate the occurrence of hot spot.

Table 2. Electrical characteristics of the PV modules as well as p^+nn^+ solar cells used to fabricate the PV modules and its class.

PV Module	I_{SC} (A)	V_{OC} (V)	FF (%)	P_{MPP} (W)	Solar cells with different rear metal grid Class of the solar cells
1	1.98	21.8	76.1	32.8	SC-grid-14%-76f class B
2	2.03	21.6	74.3	32.6	SC-grid-14%-76f class B
3	1.95	21.8	76.0	32.3	SC-grid-9%-38f class C
4	1.93	17.0	72.1	23.7	string 1: SC-grid-53%-400f string 2: SC-grid-14%-76f strings 3 e 4: SC-grid-9%-38f class B, C, D
5	1.98	21.6	75.9	32.5	string s 1 e 3: SC-grid-9%-38f string s 2 e 4: SC-grid-14%-76f class B
6	1.96	21.6	74.3	31.5	string s 1 e 2: SC-grid-14%-76f string s 3 e 4: SC-grid-53%-400f class B
7	1.93	21.3	75.6	31.1	string 1: SC-grid-9%-38f strings 2 e 3: SC-grid-14%-76f string 4: SC-grid 53%-400f class C
8	1.98	21.5	72.7	30.9	strings 1, 2, 3 e 4: SC-grid-9%-38f, SC-grid 14%-76f and SC-grid 53%-400f class A, B, C, D

As expected, in all modules the FF is higher than that of solar cells because the improvement caused by the Ag/Sn/Cu ribbon soldered on the front busbars. The I_{SC} is limited by the area of solar cells of 61.59 cm^2 and V_{OC} are compatible with the 36 series connected solar cells. From the results of the PV modules number 1, 2 and 3, any influence of the rear metal grid can be observed in the electrical parameters when the metal grid coverage is reduced from 14 % to 9 %. Modules 6 and 7 were assembled by using solar cells with metal coverage on the rear face of 53 % in some strings and the electrical characteristics of

these modules were similar to that of modules 1, 2 and 3. PV module number 4 presented a low P_{MPP} that cannot be related to the I_{SC} and this device was analyzed from the point of view of hot spots.

The electric current as a function of the applied voltage (I-V curve) of the PV module number 1 under different values of irradiance below 1000 W/m^2 is plotted in Fig. 6. The module presents a small parallel resistance of 500 Ω. This value remains practically the same for low irradiance. The shunt resistance was not clearly observed in the solar cells, as we can see in Fig. 2 and Fig. 5.

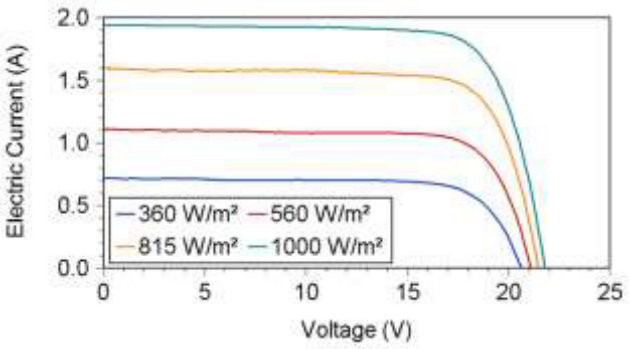

Fig. 6. I-V characteristics of the PV module number 1 assembled with p^+nn^+ solar cells under different values of irradiance.

4.2. Termographic Analysis

The thermography analysis was performed under a cloudless sky day with modules in the short-circuit condition. The solar irradiance was in the range of 500 W/m^2 - 700 W/m^2 and the angle of incidence of beam radiation was near 0°. The ambient temperature was between 27 °C and 30 °C.

The results are summarized in Fig. 7. The temperature difference between the solar cells of each photovoltaic module obtained by thermographic technique ranged from 9 °C to 18 °C.

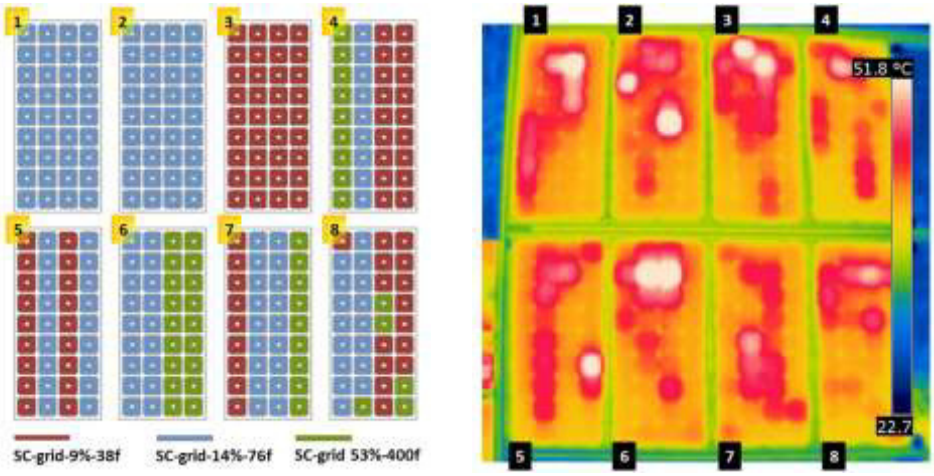

(a) (b)

Fig. 7. (a) Distribution of the solar cells with different area assembled in each PV module and (b) image thermography obtained by using an infrared camera.

All modules presented hot spots independently of the area metalized on the rear face. In the region of the electrical connection box (junction box), the temperature of the solar cells was of around 5 °C higher than that of the other solar cells, due to the reduction of heat exchange by convection.

The PV modules number 4 and 8, with lower electric power and assembled with different classes of solar cells, presented hot spots similar to that of the other modules. Then, the low open circuit voltage of (module 4) and the low fill factor (modules 4 and 8) cannot be related to soldering problems. Probably the lower V_{OC} and FF may be associated to that of the solar cells or strings.

5. Conclusions

N-type silicon solar cells with boron doped emitter processed in solar grade Czochralski (Cz) wafers with the rear area covered with Ag paste from 9 % to 53 % were fabricated and sorted. Eight PV modules were assembled using the standard process of the PV industry.

The fill factor of solar cells was lower than that expected due to the higher resistivity of the Ag/Al paste used to form the front metal grid. When the Ag/Sn/Cu ribbon was soldered on the front busbars of the solar cells the fill factor rose from 0.70 to 0.75, causing an increase in the efficiency from 13.2 % to 15.0 %.

The fill factor of solar cells was not affected by the reduction of the metal grid area on the rear face. Solar cells with rear metal coverage of 9 % and 14 % presented higher J_{SC} than the cells with a rear metal grid of 53 %.

B-emitter solar cells presented a poor response in the range of short wavelengths due to the high front recombination related to the lack of an effective passivation of the p^+ region.

The FF of the PV modules was higher than that of solar cells because the improvement caused by the Ag/Sn/Cu ribbon soldered on the front busbars. Modules presented a small shunt resistance that was not clearly observed in the solar cells.

The reduction of the metal grid area on the rear face of solar cells did not affect the fill factor of the PV modules.

The temperature difference between the solar cells of each photovoltaic module obtained by thermographic technique ranged from 9 °C to 18 °C and hot spots were not related to the area metalized on the rear face. The PV modules with lower electric power and assembled with different classes of solar cells presented hot spots similar to the other modules.

In the region of the electrical connection box (junction box), the temperature of the solar cells was approximately 5 °C higher than that of the other solar cells, due to the reduction of heat exchange by convection.

Acknowledgements

The authors gratefully acknowledge the financial support of the Brazilian financing agency FINEP (Financiadora de Estudos e Projetos) under contract n° 01.08.0635.00 and of the National Council for Scientific and Technological Development (CNPq).

References

[1] Fath P, Keller S, Winter P, Jooβ W, Herbst W. Status and perspective of crystalline silicon solar cell production. *Proc. 34th IEEE PVSC*, Philadelphia , USA, 2009; p. 2471–6.

[2] Bähr M, Dauwe S, Lawerenz A, Mittelstädt L. Comparison of bow-avoiding Al-pastes for thin, large-area crystalline silicon solar cells. *Proc. 20th EU PVSEC*, Barcelona, Spain, 2005; p. 926–9.

[3] Hering G. Enter the dragon. *Photon International*, March 2012; p. 132–161.

[4] Kopecek R, Libal J. Switch from p to n. *PV-Magazine* 06/2012; <http://www.pvmagazine.com/archive/articles/beitrag/switch-from-p-to-n-_100007072/501/#axzz2RUxJFtIL>. Accessed in 05/02/2013.

[5] Schmidt J, Bothe K, Bock R, Schmiga C, Krain R, Brendel R. N-type silicon - the better material choice for industrial high-efficiency solar cells? *Proc. 22nd EU PVSEC*, Milan, Italy, 2007; p. 998–1001.

[6] Song D, Xiong J, Hu Z, Li G, Wang H, An H, Yu B, Grenko B, Borden K, Sauer K, Roessler T, Cui J, Wang H, Bultman J, Vlooswijk AHG, Venema PR. Progress in n-type Si solar cell and module technology for high efficiency and low cost. *Proc. 38th IEEE PVSC*, Austin, USA, 2012; p. 3004–8.

[7] Cousins PJ, Smith DD, Luan HC, Manning J, Dennis TD, Waldhauer A, Wilson KE, Harley G, Mulligan WP. Generation 3: improved performance at lower cost. *Proc. 35th IEEE PVSC*, Honolulu, USA, 2010; p. 275–8.

[8] Reichel C, Granek F, Hermle M, Glunz SW. Back-contacted back-junction n-type silicon solar cells featuring an insulating thin film for decoupling charge carrier collection and metallization geometry. *Prog. Photovolt: Res. Appl.* 2012; [DOI: 10.1002/pip.2204].

[9] Woehl R, Krause J, Granek F, Biro D. 19.7 % Efficient all-screen-printed back-contact back-junction silicon solar cell with aluminum-alloyed emitter. *IEEE Electron Device Letters* 2011; **32** (3): 345–7.

[10] Kinoshita T, Fujishima D, Yano A, Ogane A, Tohoda S, Matsuyama K, Nakamura Y, Tokuoka N, Kanno H, Sakata H, Taguchi M, Maruyama E. The approaches for high efficiency HITTM solar cell with very thin (<100 μm) silicon wafer over 23 %. *Proc. 26th EU PVSEC*, Hamburg, Germany, 2011; p. 871–4.

[11] Benick J, Hoex B, Dingemanns G, Kessels WMM, Richter A, Hermle M, Glunz SW. High-efficiency n-type silicon solar cells with front side boron emitter. *Proc. 24th EU PVSEC*, Hamburg, Germany, 2009; p. 863–870.

[12] Benick J, Hoex B, van de Sanden MCM, Kessels WMM, Schultz O, Glunz SW. High efficiency n-type Si solar cells on Al_2O_3-passivated boron emitters. *Appl. Phys. Lett.* 2008; **92**:253504 [DOI: 10.1063/1.2945287].

[13] Ryu K, Upadhyaya A, Song HJ, Choi CJ, Rohatgi A, Ok YW. Chemical etching of boron-rich layer and its impact on high efficiency n-type silicon solar cells. *Appl. Phys. Lett.* 2012; **101** (7): 073902 [DOI: 10.1063/1.4746424].

[14] Mihailetchi VD, Geerligs LJ, Komatsu Y, Buck T, Röver I, Wambach K, Knopf C, Kopecek R. High efficiency industrial screen printed n-type mc-Si solar cells with front boron emitter. *Proc. 22nd EU PVSEC*, Milan, Italy, 2007; p. 1581–5.

[15] Schutz-Kuchly T, Sanzone V, Veschetti Y. N-type solar-grade silicon purified via the metallurgical route: characterisation and fabrication of solar cells. *Prog. Photovolt: Res. Appl.* 2012; [DOI: 10.1002/pip.2182].

[16] Toto S. Sanyo to mass-produce world's most efficient solar cells. *Techcrunch* 12/2010; <http://techcrunch.com/2010/12/03/sanyo-to-mass-produce-worlds-most-efficient-solar-cells/>. Accessed in 05/29/2013.

[17] Czanderna AW, Pern FJ. Encapsulation of PV modules using ethylene vinyl acetate copolymer as a pottant: a critical review. *Solar Energy Materials and Solar Cells* 1996; **43**: 101–181.

[18] Agroui K, Belghachi A, Collins G, Farenc J. Quality control of EVA encapsulant in photovoltaic module process and outdoor exposure. *Desalination* 2007; **209**: 1–9.

[19] Gautero L, Kania D, Seiffe J, Knorz A, Specht J, Nekarda J, Hofmann M, Rentsch J, Sallese JM, Preu R. Comparison of different rear contacting approaches for industrial PERC solar cells on mc-si wafer. *Proc. 25th EU PVSEC/ 5th WCPEC*, Valencia, Spain, 2010; p. 1328–1331.